A CONCEPTUAL PHOTO-ELECTRO-CHEMICAL-THERMAL (PECT) RECEIVER FOR A NET ZERO CO_2 EMISSIONS SPTC PLANT

D. D. Nation[1], P. J. Heggs[1] and D.W. Dixon-Hardy[1]
[1] ERRI, School of Process Environment and Materials Engineering
Faculty of Engineering
University of Leeds, LS2 9JT, United Kingdom

ABSTRACT

This paper outlines the conceptualization and initial modelling of a Photo-Electro-Chemical-Thermal (PECT) Receiver, a hybridization of Sodium Sulphur (NaS), Parabolic Trough Collector (PTC) and low cost Photo-voltaic Technology, for use in Concentrating Solar Plants (CSP). Visible solar radiation is converted directly to electricity for storage in NaS cells by thin film solar cells, while the Infrared and UV spectrum is absorbed into the HTF for electricity generation via a heat exchanger. The use of a PECT central receiver tube in CSP plants could result in increased plant robustness to energy demands, better overall energy utilization, and could provide a built in storage capability for PTC power plants.

1. Introduction

Renewable energy power plants in the solar thermal sector are today the largest commercial converters of solar to electrical energy in the world, currently with about 1.17GW (Wang, 2011) of global installed capacity as of 2011. Continued growth is expected with, a further 17.54 GW of global capacity soon to be commissioned.

Three main types of solar thermal plants are currently in deployment. These are Solar Power Tower (SPT), Solar Parabolic Trough Collector (SPTC), and Solar Dish-Sterling (SDS) plants. All three technologies have solar to electric conversion efficiencies (Mariyappan, 2001) greater than 20%, exceeding the commercial Photo-Voltaic market average of 11%. However, of these three, Solar Parabolic Trough (SPTC) power plants (Fig.1) are the most popular, largely because of a proven track record of performance which extends as far back as the 1980's when the first commercial plants were built.

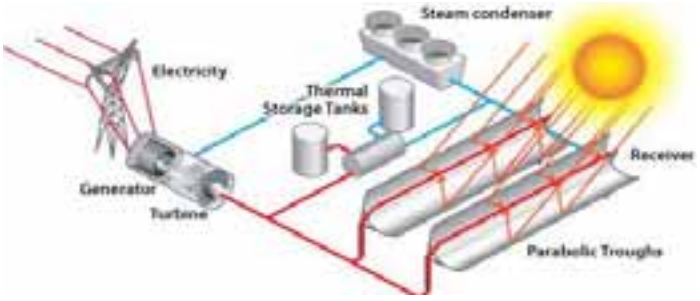

Fig. 1 - A SPTC Power Plant (Source: C&S Enterprises)

Today, SPTC plants are among the important renewable energy technologies aimed at reducing global CO_2 emissions through conversion of the sun's energy, an important factor in fighting effects of climate change. Due to the fact however, that power plants must operate 24hrs, all SPTC plants are hybrids, with fossil fuel

input from gas fired boilers (Price, 2002) providing power during night time and low sun periods.

Consequently in this paper, the authors conceptualize a PECT receiver for eliminating or significantly reducing fossil fuel usage in SPTC power plants. This could be achieved, through hybridizing the standard SPTC plant with sodium sulphur battery storage and low cost photovoltaic technology. This could one day result in a net zero CO_2 emissions plant, which with modern thermal storage (Price, 2003) would be capable of 24hr operation.

2. The conceptual hybrid system

2.1 The PECT Receiver in a SPTC – Cross Section

From a theoretical perspective, the PECT SPTC system generates power by trapping approximately 70-80% of the collected solar energy in a heat transfer fluid for electricity power generation via a traditional Rankine steam power cycle while storing most of the rest as electrochemical energy in high energy density sodium sulphur cells. Unlike the traditional system, the PECT system proposes to improve the overall electrical conversion efficiency of solar power plants by the use of spectrally selective filters (Imenes, 2006) during the solar energy conversion process.

About 75% (Forristall, 2003) of the concentrated radiation in SPTC's reaches the central absorber or HCE, where about 95% is absorbed with about 10% lost as long wave radiation. Despite good HCE absorptivity, it is seen that over 20% of the concentrated radiation is lost before it could be absorbed, of which a good portion is visible radiation. The the use of a spectral beam splitter, the PECT receiver proposes to increase the overall SPTC system efficiency by redirecting visible spectral wavelengths of 0.4 – 1.1 microns onto a narrow array of spectrally matching low cost silicon thin film cells (Fig. 2), where they can be more efficiently converted to electrical energy.

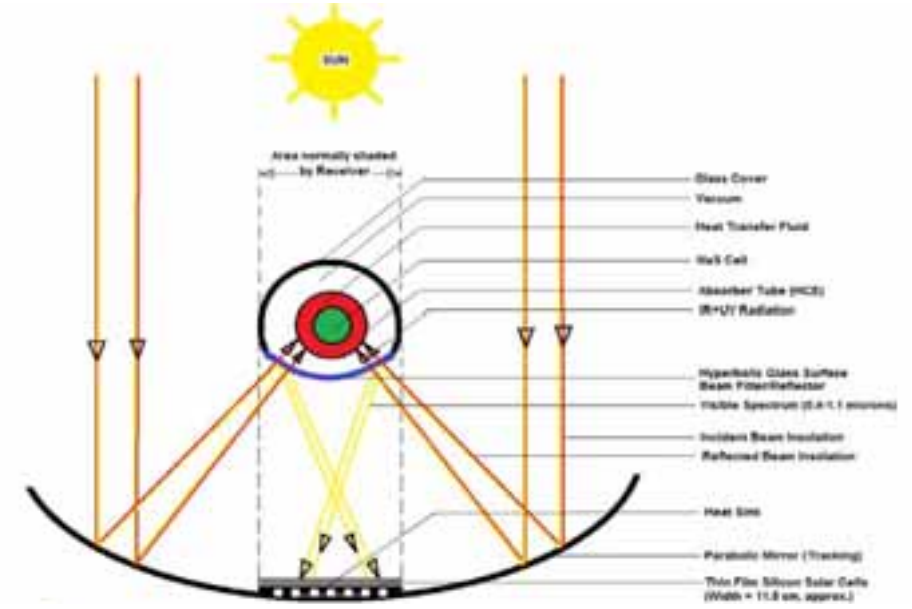

Fig. 2: The SPTC PECT System with Spectral Beam Filter

A prototype Nb_2O_5 / SiO_2 spectral filter, designed using the needle optimization method (Jiang, Wang & Jia,

2011) achieves very good spectral match with silicon solar cell response. Results show that most of the radiation inappropriate for the solar cell passes through the filter for thermal conversion by the absorber, while the 0.4-1.1 micron band is reflected away from the surface. In the PECT system the reflected visible radiation will be focused onto low cost silicon cells by the hyperbolic filter surface. The concentration of spectrally matched flux onto the cells significantly increases the cell conversion efficiency, while at the same time greatly reducing the normal thermal load due to concentration.

Another benefit is that the solar cell array is fixed along the shaded area of the mirror, thus putting to productive use traditionally wasted mirror area. The electrical energy converted by this array of cells is then used to charge the NaS cells inside the absorber tube over a 12 hour period. Sodium sulphur (NaS) cells are thermally activated cells with very high energy density and an operational temperature range of 290 – 390 °C (Sudworth & Tiley, 1985), ideally suited for the 291 - 393°C HTF loop temperature range (Forristall, 2003) of most SPTC power plants today.

In the PECT receiver, the HTF flowing in the annulus around the NaS cells is used to bring the cells to working temperature. After this is achieved, flow control, receiver focus control and heat exchange are used to maintain the desired operational temperature of the cells during charging and discharging, (Hussien et. Al, 2007) which are largely endothermic and exothermic processes respectively. The fact that NaS battery storage systems are a proven technology is evidenced by their current commercial role (Tamakoshi, 2001), in providing the electricity grid with mega-watts of continuous standby power for up to 8 hrs under full load. It is this characteristic that makes NaS cells congruent with the needs of SPTC plants during “no sun” hours and at night time.

2.2 The SPTC PECT Plant Heat Transfer Loop

Heat transfer analysis is carried out on a SPTC loop, (Fig. 3) the basic building block of all SPTC plants. The operational parameters chosen are similar to the LUZ-3 plant, an industry standard, with average inlet and outlet temperatures of 290°C and 390°C respectively.

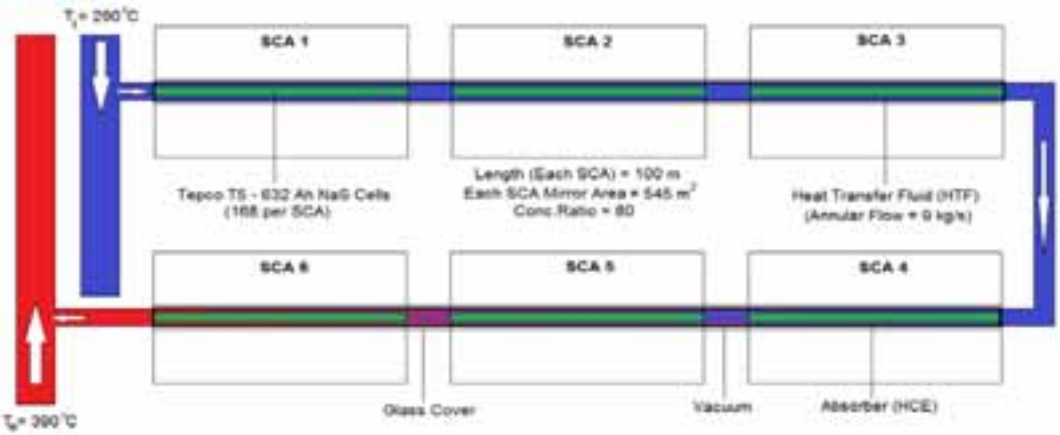

Fig. 3: Simplified SPTC PECT Loop

2.3 Conceptual Thermal Management of NaS cells

Before the NaS cells can be charged or discharged, they must be brought up to operational temperature. This is the first function of the HTF fluid circulating in the annulus. The working temperature range of the NaS cells is 290 – 390 °C (Sudworth & Tiley, 1985) almost identical to the LUZ-3 HTF loop temperature profile of 291 - 393°C. Once the plant has reached operating temperature the NaS cells will operate in one of 3 modes

a) Charging Mode b) Discharging Mode c) Standby Mode

Charging Mode

Charging of the NaS cells will be spread over the 12 "sun" hours available during daylight, at a low rate compared to the discharge rate. During charging the NaS cell generates *'Resistance or Joule'* heating due to current flow through its internal resistance, and *'Endothermic Heat'* due to reverse cell reaction. When charging, resistance heat generation is slightly less than the endothermic heat absorption, (Hussien et. al, 2007), which would tend to produce a gradual fall in cell temperature over time. However, if the receiver is kept focused on incident solar flux, this fall in temperature will not occur.

This makes the charging mode one of the most challenging with respect to thermal management, Once the NaS cells have been brought up to temperature for charging, the NaS cell temperature must be maintained within the 290 – 390 °C range to prevent cell rupture. This can be done in two ways. Firstly the SCA's can be defocused intermittently, or secondly, the NaS can be cooled by switching in an annular HTF stream at a lower temperature as required. The second option is favoured by the authors since it saves the solar energy lost by a defocused SCA, along with the mechanical energy used to defocus the SCA. The energy captured by the HTF annular streams converted to the electrical power by a Rankine steam power cycle, provides the day-time electrical output of the plant, while the NaS cells are on charge. An electronic thermal control system would be required to manage the switching of NaS cooling streams by monitoring HTF loop inlet and outlet temperatures, from which NaS cell temperatures can be deduced. Calculations and model validation of these propositions will be the subject of future work.

Discharging Mode

The discharging of the NaS cells is a highly exothermic process, due to the fact that the chemical cell reaction itself is exothermic during discharge, and more importantly due to the significant resistance heating which occurs at the anticipated high discharge current rates. One benefit however is that the system will be operated in discharge mode during nightime hours, when there is no solar flux impinging the receiver, and when there is significant natural nightime cooling via the ambient, especially in desert locations. With no incident solar flux, the ($\dot{M}$Cp) of the circulating HTF will be adequate to absorb generated heat and maintain NaS cell temperatures. Model validation of this concept will also be the subject of future work. It is important to note that one major benefit of NaS cell discharge mode is the ability of the cell reaction enthalpy to maintain cell operating temperature without external heat.

Standby Mode

In standby mode the NaS cells are neither charging nor discharging, which means that they are producing neither joule nor entropic heating. However their cell temperature must be maintained by use of the circulating HTF streams.

3. Heat transfer analysis

Three operational states are now analyzed: (a) Plant transition to operating temperature (b) Plant operation during battery charging (c) Plant operation during battery discharging

3.1 Plant transition to operating temperature

We begin the by considering the PECT receiver under the following initial conditions which provide a good estimate of potential plant operation. The site of the Andasol SPTC Plant in Spain is used as a benchmark. Initial conditions:[T_{amb} = 20°C; T_{sky} = 10°C ; Solar time = 9 am; $T_{NaS} = T_{HTF} = T_{abs} = T_{amb}$; Loc. 37°N, 3°W; Month = July; *n* (Day of year) = 198; Altitude = 1100 m δ = 21.2 (Duffie & Beckman, 1991)]

Using the initial conditions above, the clear sky normal beam insolation (I_{cnb})

$$I_{cnb} = G_{sc}\tau_b = G_{sc}\left[a_0 + a_1 \exp\left(-\frac{k}{\cos\theta_z}\right)\right] \text{ W/m}^2 \quad (1)$$

where a_0, a_1 and k are adjusted for a mid-altitude summer using the Hottel (1976) correction. (Duffie & Beckman, 1991). Therefore:

$$I_{cnb} = 1367\left[0.22 + 0.67\exp\left(-\frac{0.314}{\cos 85.8°}\right)\right] \text{W/m}^2 = 1367 \times 0.232 = 317.14 \text{ W/m}^2$$

The energy balance equations along the PECT receiver cross section (Fig. 4) are as follows:

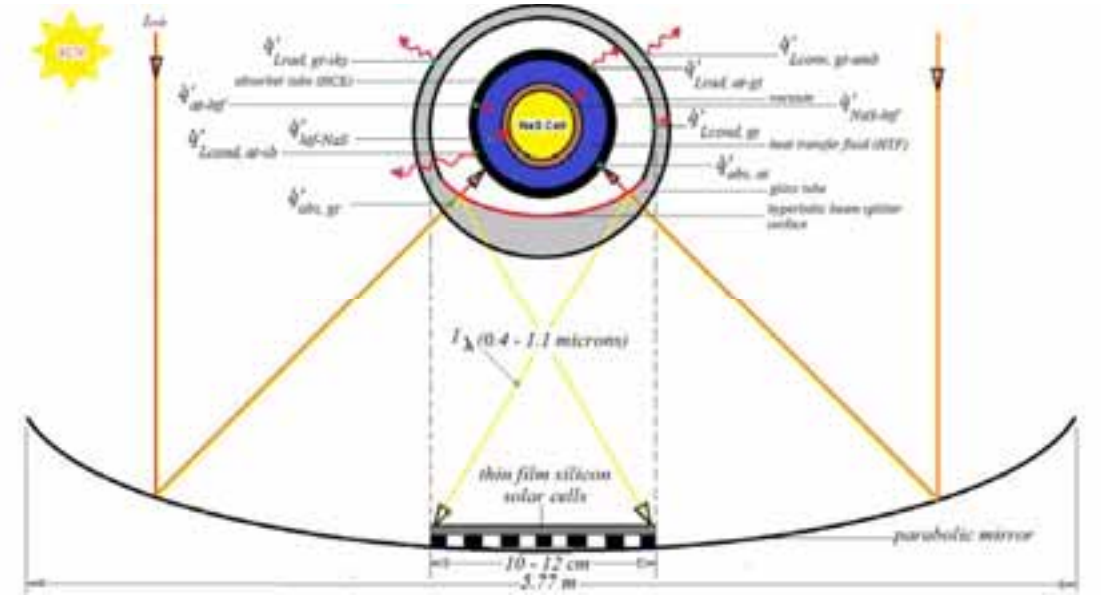

Fig.4 Heat transfer – PECT receiver cross section

At NaS cell tube (heat flow into NaS cells = +ve; from NaS cells = -ve)

(1)

$$\dot{q}_{Nas} = \dot{q}_{htf-Nas} + \dot{q}_{Nas,Gen}$$

where $\dot{q}_{Nas} = \frac{m_{Nas} c_{p,Nas}}{L(T_{Nas,o} - T_{Nas,i})}$; $\dot{q}_{htf-Nas} = h_{t,a} \pi D_{Sto,o} (T_{HTF,m} - T_{Nas,o})$, and

$\dot{q}_{Gen,Nas} = \frac{I}{L}\left[IR_{DC} + T_{Nas,t}\frac{dE}{dT}\right]$ both I and $T_{Nas,t}\frac{dE}{dT}$ being +ve for discharge, −ve for charge.

At heat transfer fluid (HTF) (heat flow into HTF = +ve; from HTF = -ve)

$$\dot{q}_{htf} = \dot{q}_{at-htf} \quad \dot{q}_{htf-Nas} \tag{2}$$

where $\dot{q}_{htf} = \frac{\dot{M} c_{p,HTF}}{L}(T_{HTF,i} - T_{HTF,o})$; $\dot{q}_{at-htf} = h_{o,a} \pi D_{at,i} (T_{at,i} - T_{HTF,m})$ and

$\dot{q}_{htf-Nas} = h_{t,a} \pi D_{st,o} (T_{HTF,m} - T_{Nas,o})$

At absorber tube (Assuming vacuum between absorber and glass tube)

$$\dot{q}_{cond,at} = \dot{q}_{at-htf} \tag{3}$$

$\dot{q}_{cond,at} = \frac{2\pi k_{at}(T_{at,o} - T_{at,i})}{\ln\left[\frac{D_{at,o}}{D_{at,i}}\right]}$ and $\dot{q}_{at-htf}$ $h_{o,a} \pi D_{at,i} (T_{at,i} - T_{HTF,m})$

where

$$\dot{q}_{abs,at} = \dot{q}_{cond,at} + \dot{q}_{rad,at-gt} + \dot{q}_{Lconv,at-sb} \tag{4}$$

where $\dot{q}_{abs,at} = \frac{\dot{q}''_{sol} \times A_{col} \times \rho_m (\tau_{gt} \alpha_{at} \gamma) K_{\tau\alpha\gamma}}{L}$; $\dot{q}_{cond,at} = \frac{2\pi k_{at}(T_{at,o} - T_{at,i})}{\ln\left[\frac{D_{at,o}}{D_{at,i}}\right]}$ and

$$\dot{q}_{rad,at-gt} = \frac{2\pi\sigma\left(T_{at,o}^4 - T_{gt,i}^4\right)}{\left[\frac{1}{F_{at,gt}} + \left(\frac{1}{\varepsilon_{at}} - 1\right) + \frac{D_{at,o}}{D_{gt,i}}\left(\frac{1}{\varepsilon_{gt}} - 1\right)\right]^{-1}}$$

and $\dot{q}_{Lconv,at-sb} = \left(\frac{\sqrt{\bar{h}_b F_b k_b}(T_{sb} - T_{amb})}{L}\right)^{\circ}$ (*Incropera and Dewitt, 1990)

At glass tube (Assuming vacuum between absorber and glass tube)

$$\dot{q}_{rad,at-gt} = \dot{q}_{Lcond,gt} \tag{5}$$

$\dot{q}_{Lcond,gt} = \frac{2\pi k_{gt}(T_{gt,i} - T_{gt,o})}{\ln\left[\frac{D_{gt,i}}{D_{gt,o}}\right]}$

where

$$\dot{q}_{Lcond,gt} + \dot{q}_{abs,gt} = \dot{q}_{rad,gt-sky} + \dot{q}_{Lconv,gt-amb} \tag{6}$$

where $\dot{q}_{abs,gt} = \frac{\dot{q}''_{sol_{const}} \times A_{col} \times \rho_m \tau_{gt} K}{L}$; $\dot{q}_{rad,gt-sky} = 2\pi r \varepsilon_{gt} \left(T_{gt,o}^4 - T_{sky}^4\right)$

$$and\ \dot{q}''_{Lconv,gt-amb} = 2\pi h_w (T_{gtw} - T_{amb})$$

A few of the important parameters in this system have been solved s solved using LabVIEW and MS Excel software, and can be found in the results section.

3.2 NaS cell energy storage calculations (based on a LUZ-3 plant industry standard)

Each SCA contains 168 T5 Tepco NaS cells, each cell with 632 Ah capacity and Emf = 2V.

- ⇨ Total electrical storage capacity/SCA = IVt = 632Ah × 2V × 168 cells = 212.352 kWh

Each Plant Loop contains 6 SCA's

- ⇨ Total electrical storage capacity/Plant Loop = No. SCA's/Loop × SCA Capacity
- ⇨ = 212.352 × 6 = 1.274 MWh

Each Plant contains 142 Loops

- ⇨ Total electrical storage capacity of Plant = 1.274 MWh/Loop × 142 Loops = 180.92 MWh

If the number of "no-sun" hours = 12, for a plant with the standard 6hrs of thermal storage, the other 6hrs of energy output could be provided by the NaS cells.

Output = Capacity/No. of hrs = 180.92 MWh/6hrs = 30.15 MWe.

Thus, a 30MWe PECT SPTC plant with a LUZ-3 footprint and 6hrs thermal storage could theoretically operate without fossil fuel input, provided the combination of NaS cells and thermal storage can power the plant for 12 "no-sun" hours.

One advantage with the PECT system is that the energy stored in the NaS cells is already 'electrical energy'. With the required power inverters as used in the Japanese and US power grids (Kamibayashi, 2001), the energy can be delivered to the grid on demand.

3.3 Potential of photo-voltaic energy generation

Each SCA has a useful mirror area of 545 m^2. At an average daily direct normal beam insolation of 500W/m^2:

- ⇨ Solar energy collected per SCA every second = 545 m^2 × 500 W/m^2 = 272.5 kW
- ⇨ Solar energy collected per loop every second = 272.5kW × 6 SCA's = 1.64 MW
- ⇨ Solar energy collected by plant every second = 1.64 × 142 loops = 232.88 MW

With the beam splitter delivering 10% (selected wavelength) of this energy to the solar cells:

- ⇨ Energy incident on solar cells = 23.29 MW

  Assuming a cell conversion efficiency of 50% (the rest is converted to heat, which can be collected) because of good spectral match, energy converted to electricity would be:
- ⇨ 0.5 x 23.29 MW = 11.65 MW
- ⇨ Time taken to recharge plant storage capacity of 180 MWh = 180MWh/11.65MW = 15.46 hrs.

  Therefore 12 sun hours of charging should still be adequate since manufacturer recommendations are to limit discharge of NaS batteries to 80% of capacity in each discharge cycle for longer service life.

4. SOME SIMULATED RESULTS

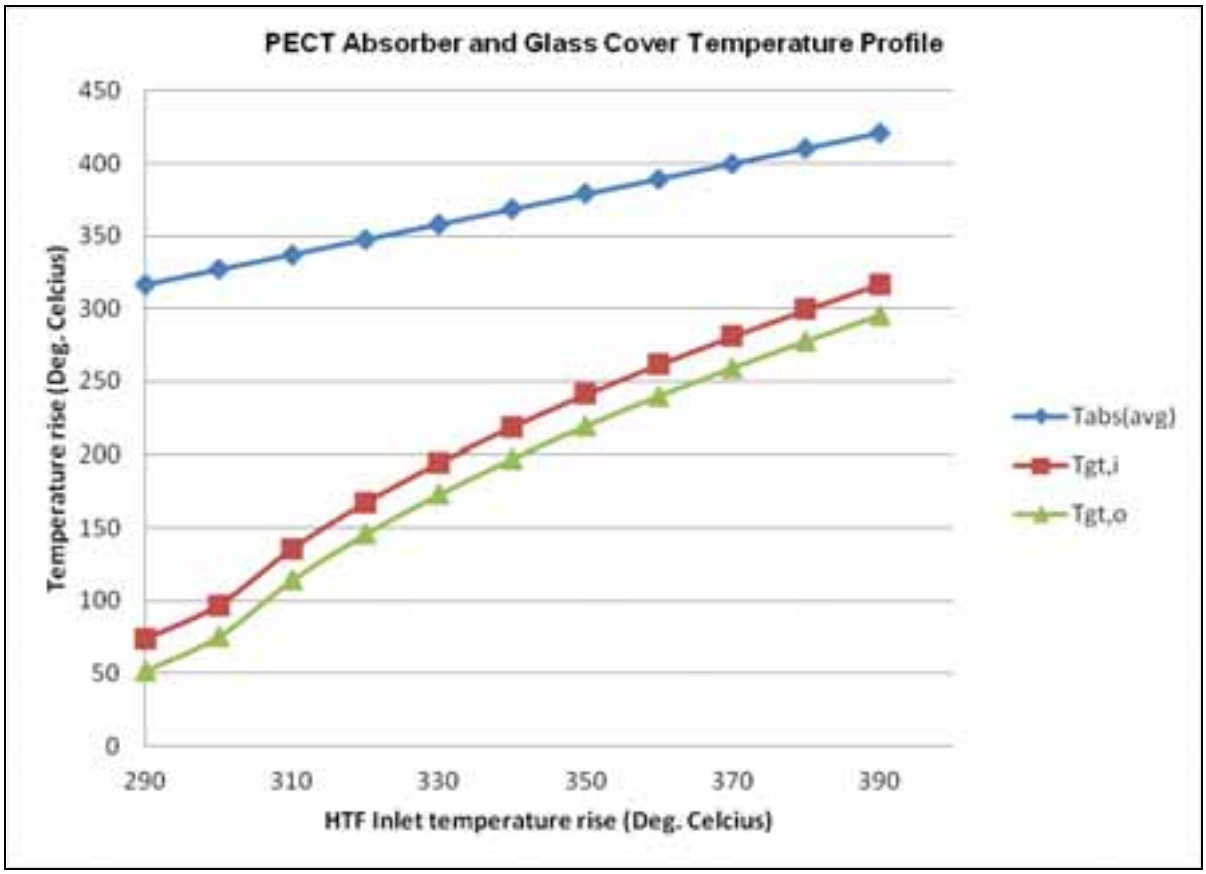

Fixed parameters: Solar insolation : 1000W/m^2; Mass flow = 9kg/s

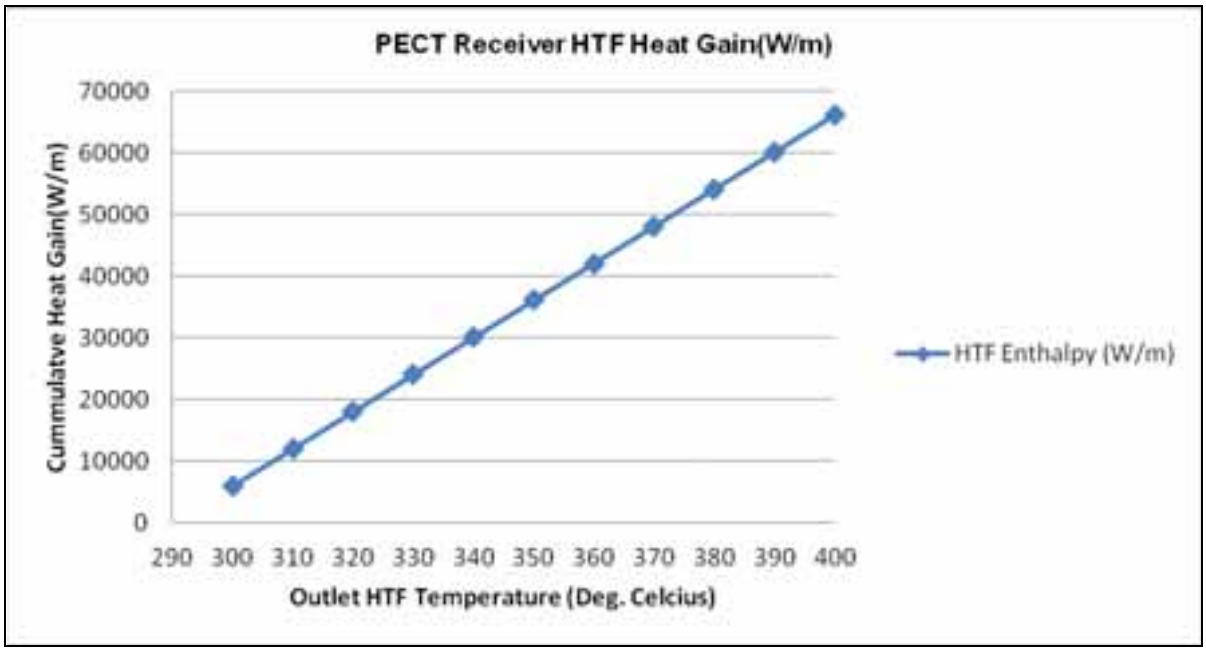
PECT Receiver HTF Heat Gain(W/m)
Cummulatve Heat Gain(W/m)
70000
60000
50000
40000
30000
20000
10000
0
290 300 310 320 330 340 350 360 370 380 390 400
Outlet HTF Temperature (Deg. Celcius)
HTF Enthalpy (W/m)

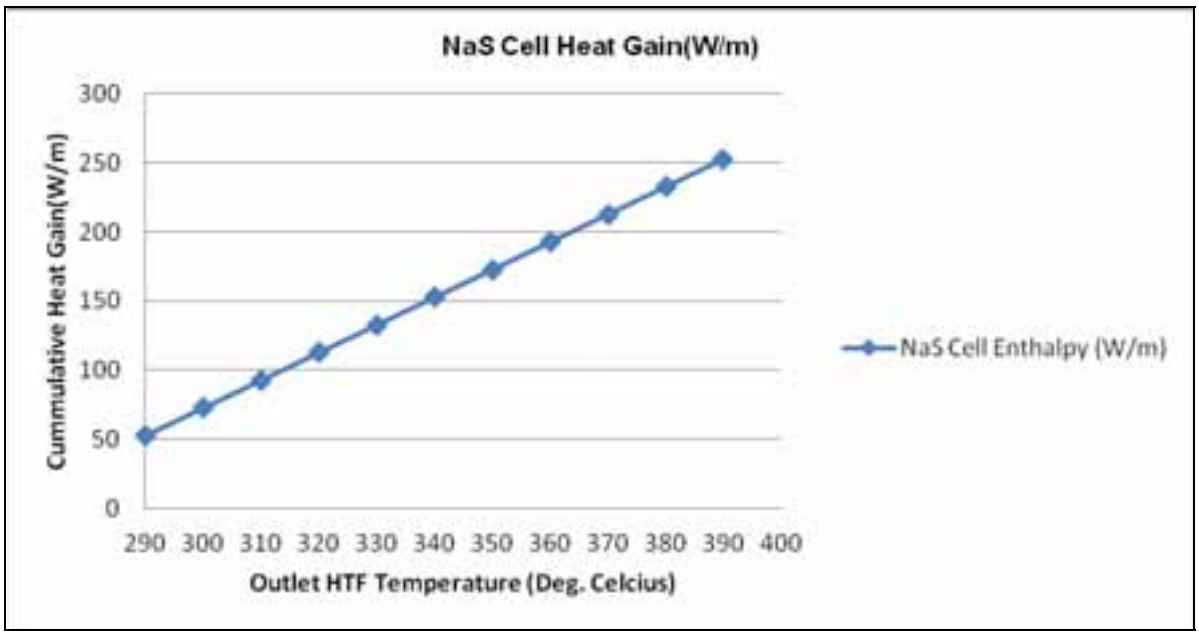
NaS Cell Heat Gain(W/m)
Cummulative Heat Gain(W/m)
300
250
200
150
100
50
0
290 300 310 320 330 340 350 360 370 380 390 400
Outlet HTF Temperature (Deg. Celcius)
NaS Cell Enthalpy (W/m)

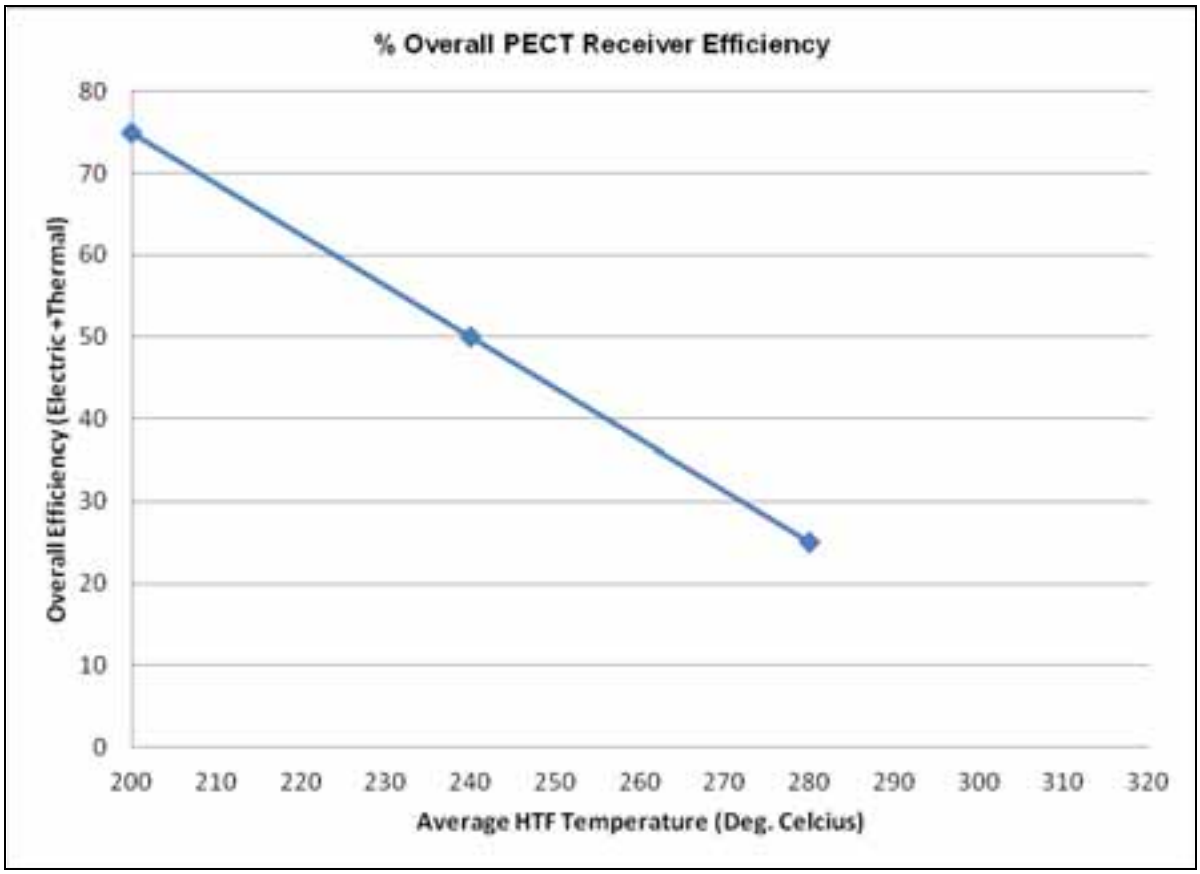

%Eff. = [(Thermal +Electrical Output)/ Collected Solar Beam Radiation]x 100

5. FUTURE WORK

After a steady state analysis of the PECT plant is to be carried out with the model described in this paper, a transient model of the system needs to be constructed in order to determine how the system will function under the dynamic charge/discharge conditions. Also the operation of the solar cells under the normal SPTC plant concentration ratios of 40 – 80 suns, their conversion efficiency gains, and the effectiveness of the spectral beam filter will be investigated through appropriate modelling.

6. CONCLUSION

In this paper a steady state model for a PECT SPTC receiver has been presented. Preliminary calculations suggest that the PECT concept of hybridizing SPTC, Photo-Voltaic and NaS storage technology could lead to an elimination of fossil fuel usage in SPTC plants, from an energy generation perspective. Should further analysis confirm the feasibility of this concept through power plant efficiency gains, adopting the PECT receiver into existing SPTC plants could see a significant reduction in CO_2 footprint and provide the plant with an inherent capacity to store electricity. This facility does not exist currently.

7. NOMENCLATURE

c_{pHTF}	Specific heat capacity of Heat Transfer Fluid	$\left(\frac{J}{kgK}\right)$
$D_{gt,o}$	External diameter of Glass tube	(m)
$D_{gt,i}$	Internal diameter of Glass tube	(m)
$D_{at,o}$	External diameter of absorber tube	(m)
$D_{at,i}$	Internal diameter of absorber tube	(m)
$F_{at,gt}$	View factor between absorber and glass tube	(unitless)
h_{conv}	Convective heat transfer coefficient over glass tube	$\left(\frac{W}{m^2K}\right)$
$h_{an,o}$	Annular heat transfer coefficient from absorber tube to HTF	$\left(\frac{W}{m^2K}\right)$
$h_{an,i}$	Annular heat transfer coefficient from HTF to NaS battery tub	$\left(\frac{W}{m^2K}\right)$
k_{HTF}	Thermal conductivity of heat transfer fluid	$\left(\frac{W}{mK}\right)$
$K_{\gamma\tau\alpha}$	Incidence angle modifier	(unitless)
L	Unit length of PECT module	(m)
$\dot{M}$	Mass flow rate of HTF	$\left(\frac{kg}{s}\right)$
Nu	Nusselt number	(unitless)
Pr	Prandtl number	(unitless)
$\dot{q}'_{abs,at}$	Heat flux absorbed by absorber tube per unit length	$\left(\frac{W}{m}\right)$
$\dot{q}'_{at-htf}$	Heat flux from absorber tube to heat transfer fluid per unit ler	$\left(\frac{W}{m}\right)$
$\dot{q}'_{cond,at}$	Heat flux conducted through absorber tube per unit length	$\left(\frac{W}{m}\right)$
$\dot{q}'_{cond,NaS}$	Heat flux conducted through NaS cell per unit length	$\left(\frac{W}{m}\right)$
$\dot{q}_{htf}$	Heat energy of heat transfer fluid per unit length	$\left(\frac{W}{m}\right)$
$\dot{q}'_{htf-NaS}$	Heat flux from heat transfer fluid to battery tube per unit leng	$\left(\frac{W}{m}\right)$
$\dot{q}'_{Lcond,at-sb}$	Conductive heat loss from absorber tube to support bracket per unit length	$\left(\frac{W}{m}\right)$
$\dot{q}'_{Lcond,gt}$	Conductive heat loss through glass tube per unit length	$\left(\frac{W}{m}\right)$
$\dot{q}'_{Lconv,gt-amb}$	Convective heat loss from glass tube to ambient per unit lengt	$\left(\frac{W}{m}\right)$
$\dot{q}'_{Lrad,at-gt}$	Radiative heat loss from absorber tube to glass tube per unit length	$\left(\frac{W}{m}\right)$
$\dot{q}'_{Lrad,gt-sky}$	Radiative heat loss from glass tube to sky per unit length	$\left(\frac{W}{m}\right)$
$\dot{q}'_{NaS-htf}$	Heat flux from NaS cells to heat transfer fluid per unit length	$\left(\frac{W}{m}\right)$
$(q'')_{sol}$	Direct normal solar flux	$\left(\frac{W}{m^2}\right)$
Re	Reynolds number	(unitless)
T_{amb}	Temperature of ambient	(K)
$T_{at,o}$	Outer temperature of absorber tube	(K)
$T_{at,i}$	Inner temperature of absorber tube	(K)
$T_{gt,o}$	Outer temperature of glass cover	(K)
$T_{gt,i}$	Inner temperature of glass cover	(K)
$T_{HTF,m}$	Mean heat transfer fluid temperature	(K)
$T_{NaS,i}$	Inner temperature of NaS cell	(K)
$T_{NaS,o}$	Outer temperature of NaS cell	(K)

8. REFERENCES

Beckman, W.A., Duffie, J. A., 1991. Solar Engineering of Thermal Processes. second ed., Wiley, New York.

Cohen, G., 1993. Operation and efficiency of large-scale solar thermal power plants. In Proceedings of Optical Materials Technology, Energy Efficiency and Solar Energy Conversion, SPIE, Vol. 2017, p. 332-337.

Forristall, R., 2003. Heat transfer analysis and modelling of a parabolic trough solar receiver implemented in engineering equation solver. Technical Report, NREL/TP-550-34169, Prepared under Task No. CP032000 National Renewable Energy Laboratory(NREL), Department of Energy, USA.

Garcia-Valladares, A., Velazquez, N., 2008. Numerical simulation of parabolic trough solar collector: Improvement using counter flow concentric circular heat exchangers. International Journal of Heat and Mass Transfer 52 (2009) 587-609

Kays, W.M., London, A.L., 1984. Analytical solutions for flow in Tubes, in: Compact Heat Exchangers. Krieger Pub. Co., pp. 115 -125

Kearney, D., Price, H., 2005. Advances in parabolic trough solar power technology. Advances in Solar Energy. Vol. 16, Kreith, F., Goswami, D.Y. (Eds.), ASES, Boulder, Colorado, 2005

Mariyappan, J., Anderson, D., 2001. Solar thermal thematic review. Draft Report., The Global Environment Facility (GEF) Washington, DC., USA

Odeh, S.D., Morrison, G.L., Behnia, M., 1998. Modelling of Parabolic Trough Direct Steam Generation Solar Collectors. Solar Energy, Vol. 62, No. 6, p. 395-406

Price, H., et.al., 2002. Advances in parabolic trough solar power technology. Journal of Solar Energy Engineering, Vol. 124, May 2002, 109-125

Price, H., 2003. A parabolic trough solar power plant model simulation model. ISES 2003 Conference Report Preprint, National Renewable Energy Laboratory, 1617 Cole Blvd., Golden, Colorado, 80401, USA

Rolim, M.M., Fraidenraich, N., Tiba, C., 2008. Analytic modelling of a solar power plant with parabolic linear collectors. Solar Energy 83 (2009) 126-133

Sudworth, J.L., Tiley, A.R., 1985. The Sodium Sulphur Battery. University Press, Cambridge, Great Britain

Tamakoshi, T., 2001. Recent sodium sulphur battery applications in Japan. A presentation at the ESA 2001 Annual Meeting, April 26-27, 2001, Chattanooga, Tennessee, USA

WEB REFERENCES

Hussein, Z., et. al., 2007. Modeling of sodium sulphur battery for power system applications. Elektrika. Vol. 9, No.2, 2007, 66-72 . Retrieved August 9, 2011 from www.fke.utm.my/elektrika/dec07/paper11dec07.pdf

Wang, U., 2011. The rise of concentrating solar thermal power. Press Release., July 14, 2011., The Global Energy Network Institute. Retrieved August 9, 2011 from http://www.geni.org/globalenergy/library/technical-articles/generation/renewableenergyworld.com/the-rise-of-concentrating-solar-thermal-power/index.shtml